Molecular Crystals and Liquid Crystals

Publication details, including instructions for authors and subscription information:
http://www.tandfonline.com/loi/gmcl20

Amazing Pores: Processing, Morphology and Functional States of Molecularly Imprinted Polymers as Sensor Materials

Joseph J. BelBruno [a] , Asta Richter [b] & Ursula J. Gibson [c]

[a] Center for Nanomaterials Research and Department of Chemistry, Dartmouth College, Hanover, NH, USA

[b] Department of Engineering Physics, University of Applied Sciences Wildau, Wildau, Germany

[c] Center for Nanomaterials Research and Thayer School of Engineering, Dartmouth College, Hanover, NH, USA

Version of record first published: 16 Jun 2008

To cite this article: Joseph J. BelBruno, Asta Richter & Ursula J. Gibson (2008): Amazing Pores: Processing, Morphology and Functional States of Molecularly Imprinted Polymers as Sensor Materials, Molecular Crystals and Liquid Crystals, 483:1, 179-190

To link to this article: http://dx.doi.org/10.1080/15421400801905135

Mol. Cryst. Liq. Cryst., Vol. 483, pp. 179–190, 2008

ISSN: 1542-1406 print/1563-5287 online
DOI: 10.1080/15421400801905135

Taylor & Francis
Taylor & Francis Group

Amazing Pores: Processing, Morphology and Functional States of Molecularly Imprinted Polymers as Sensor Materials

Joseph J. BelBruno[1], Asta Richter[2], and Ursula J. Gibson[3]
[1]Center for Nanomaterials Research and Department of Chemistry, Dartmouth College, Hanover, NH, USA
[2]Department of Engineering Physics, University of Applied Sciences Wildau, Wildau, Germany
[3]Center for Nanomaterials Research and Thayer School of Engineering, Dartmouth College, Hanover, NH, USA

Molecularly imprinted polymers function as synthetic antibodies, binding with specificity to a molecule of a particular shape or exhibiting a specific functional group. The polymers may be applied to numerous fields of research including separations, drug delivery and sensors. In this review, we describe the general properties of imprinted polymers, several production techniques and physical and morphological characteristics, especially for thin films. Particular focus is made with respect to functional states of imprinted polymers and their application as the active component of sensing devices.

Keywords: AFM; imprinted polymer; nanoindentation; sensors; thin films

INTRODUCTION

Imprinted polymeric materials were initially developed as analytical materials intended to provide molecule specific separations by chromatography [1] or solid phase extraction [2]. The antibody-like nature of these materials has provided researchers with numerous other applications including drug delivery [3], library screening [4], chiral separations [5], purification [6], nanoreactors [7], biomimetic materials [8] and sensing elements [9]. Here, we provide a brief exposition

Address correspondence to Joseph J. BelBruno, Center for Nanomaterials Research and Department of Chemistry, Dartmouth College, Hanover, NH 03755, USA. E-mail: jjbchem@dartmouth.edu

on the basics of molecularly imprinted polymer (MIP) chemistry, a survey of the applications and a focus on the physical and morphological properties of these materials, especially as applied to their application to sensing devices.

Antibodies are natural materials produced to recognize antigens and direct both therapeutics and separations of biological molecules. Unfortunately, antibodies are proteins and are easily denatured under relatively mild conditions. MIPs, on the other hand, act as synthetic antibodies; they possess the ability to recognize and bind specific target, not only biological, molecules. In addition to near universality in terms of target, MIPs offer another distinct advantage over natural receptors; because they are polymers, they are robust and can survive challenging experimental conditions.

The basic MIP concept in shown in Figure 1. Functional monomers self-assemble around a template molecule and are subsequently cross-linked into place. Under defined conditions, the template can be removed, leaving behind a cavity complementary in shape and functionality, which will bind molecules identical to the template. The imprint functions like a lock that is only compatible with the correct key. The template molecule may be bound either covalently or non-covalently with each option providing advantages and disadvantages. Covalently bound MIPs provide homogeneous binding sites and the template is less easily displaced once it is in the cavity. However, this stronger binding means that both template removal after production and rebinding in the application are slow, limiting the potential as a sensing element. Non-covalent MIPs are less homogenous in terms of cavity properties, but the weaker binding that results from, for example hydrogen bonding forces, means that template activity within the cavity is relatively rapid. Most applications, and certainly sensing applications, rely more heavily on these types of materials.

FIGURE 1 A MIP with the imprint molecule present (starting at the left side), removed leaving behind the receptor site and selected from a mixture of possible molecules.

MIP PREPARATION

Most MIPs are prepared from monomeric materials. Typical MIP systems [10] involve polymerization of a monomer (for example, MAA) and cross-linker (EGDM) with photoinitiator (AIBN) in the presence of the template. After polymerization, the template is removed and the polymer exhibits the ability to recognize and bind to template molecules with a high degree of selectivity. A phase inversion method may also be employed [11,12]. In this technique, polymeric material is dissolved in a theta solvent along with the template molecule and a polymer-template network is established in solution. The imprinted polymer may be precipitated by addition of a poor solvent to the theta solution. Alternatively, and for our purposes, the theta solution may be used to spin coat thin (several μm to tens of nm) MIP films onto almost any substrate [13,14].

Spin coating is a simple deposition process in which the casting solution, a dissolved polymer-template network, is dropped onto the substrate, which is rotated at high speed. This rotation spreads the solution evenly over the surface and also causes most of the solvent to evaporate leaving a thin MIP film on the substrate. The substrate is usually baked immediately after spin casting to remove the remaining solvent in the film. With this technique, any solvent left trapped in the MIP film will detrimentally affect its performance. Films are quite stable and generally may be stored or used for an indefinite time.

Casting solutions are covered, but not air purged, and stirred at room temperature for 24 hours. Films are spin cast from these solutions onto, for example, glass microscope cover slips. Film adhesion is an important property and careful treatment of the substrate is required. Typically, substrates are prewashed in concentrated nitric acid and cleaned with spectroscopic grade isopropanol and acetone prior to polymer deposition. The films are sensitive to the composition/viscosity of the solution and the rotational speed of the substrate. The spin coater is operated at several speeds, depending upon the viscosity of the solvent, from 2000 rpm up to 9000 rpm for 30s-60s with negligible ramp up time. The process of film production from spin coating involves a balance between the viscosity of the coating solution and the evaporation rate of the solvent. The physical nature of the polymerization (producing crystalline or amorphous films, or a mixture) is dependent on the speed of the solvent evaporation. The concentration of polymer in the solution is the dominant variable for the film thickness. Films can be grown with just a few molecular layers up to a few μm in thickness. At the lowest concentrations, the practical limitation on the minimum film thickness is adhesion to the substrate.

NANOMECHANICAL AND MORPHOLOGICAL PROPERTIES

Morphology of the films is template-dependent, but is also associated with the polymer and the initial functional state [15]. Figure 2 presents AFM results for three different MIP systems. In general, the presence of the template molecule, as opposed to the production of a control film without the template, yields a complex structure. In the case of nylon-glutamine, Figure 2a, the control film exhibits a mixed crystalline-amorphous morphology, while the imprinted material, with either of two different amino acids, has a porous structure. The PVP-fructose MIP, Figure 2b, is sponge-like in appearance, while the corresponding control is nearly absent structural features. Finally, a control PVP film is compared with a MIP containing 4-methyl nitrobenzoate in Figure 2c. The morphology difference is striking, as a complex, fractal-like structure is observed in the latter case. Closer analysis indicates that pores are present beneath the surface structure shown in

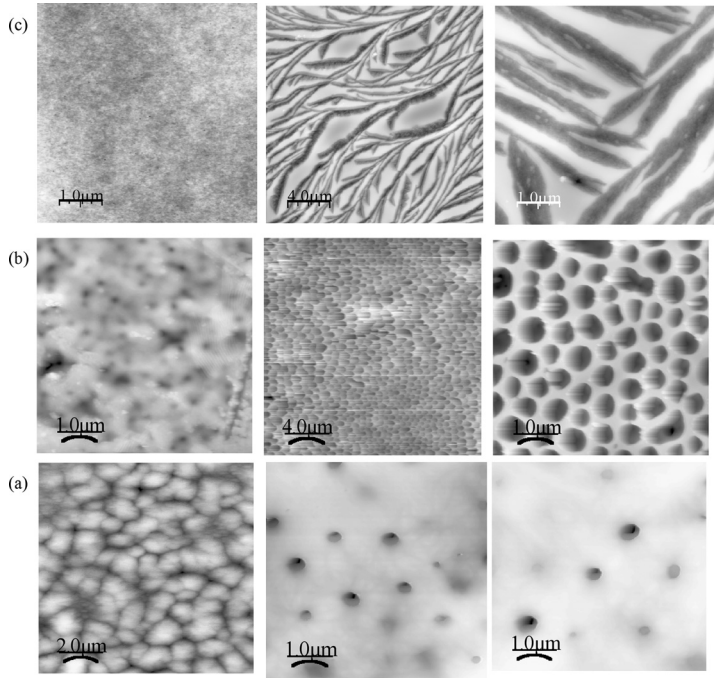

FIGURE 2 Morphology comparison for control and imprinted films at various AFM resolutions: (a) Nylon control; alanine imprinted and glutamine imprinted; (b) Polyvinylphenol control and fructose imprinted and (c) Polyvinylphenol control and 4-methyl nitrobenzoate imprinted.

the figure. The structure of the imprinted films is characteristic and persistent, even if one removes the template from the film. Some such films have been cycled through the template removal-template reintroduction sequence up to ten times. Three functional states of imprinted polymers may be defined: the *as created* state in which the template molecule still resides within the newly created cavity, the *empty* state in which the template molecule has been removed, leaving behind the vacant binding site and the *reinserted state*, in which the template molecule has been extracted from a solution or the ambient vapor and reinserted into the cavity. If these states can be identified by nanomechnical properties, then attributes such as hardness may be used as a reporting mechanism for the rebinding process in the thin films.

Nanoindentation [16] is the ideal technique for the determination of nanomechanical properties for polymers and other materials that are not homogeneous in depth. MIPs clearly fall into such a category. In these experiments, load, F, and depth, h, are recorded simultaneously. The depth-dependent force function, $F(h)$, yields the hardness and the elastic modulus. Typically, a dedicated nanoindentor such as the Hysitron UB1 Triboscope [17] with a 90° diamond corner cube is used to make the measurements. The main operating element of such a device is a three-plate capacitor, with the indentation diamond attached to the mid-plate. A DC voltage is then applied to drive the diamond tip into the sample. Capacitance changes are measured as a function of applied voltage and converted into F vs. h plots, leading to a $F(h)$ curve. The loading curve contains effects of both elastic and plastic deformation, while the unloading curve is assumed to be reflective of only elastic properties [18]. Each point of the loading curve corresponds to a hardness value. If the contact depth as a function of penetration from the loading curve is fit to a function, $h_c(h)$, then the contact area, $A_c(h_c(h))$, is determined and the hardness as a function of depth is calculated by

$$H(h) = \frac{F(h)}{A_c(h)} \tag{1}$$

and the indentation modulus is given as

$$E = 0.5\left(\frac{dF}{dH}\right)\left(\frac{1}{(A_C/\pi)^{0.5}}\right). \tag{2}$$

The ideal way to collect the nanomechanical properties as depth-dependent data is to use multicycling; perform a series of loading/unloading cycles in one experiment and at a single position

on the film. A 12-cycle nanoindentation sequence with parabolically increasing applied F_{max} is shown in Figure 3a. The experimental result of applying such a sequence is 12 data sets relating actual force, penetration depth, contact area, etc., from a set of curves such as that shown partially in Figure 3b for a nylon control sample. Using Eq. (1),

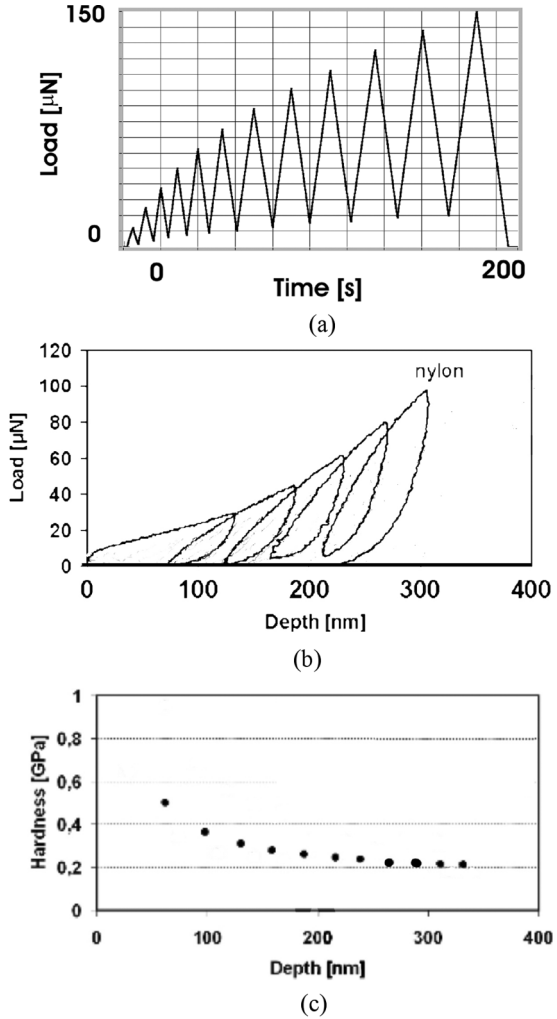

FIGURE 3 A 12 cycle load-time curve (a) applied to a nylon control sample, the corresponding partial force-depth curve (b) and the calculated nanohardness as a function of depth (c).

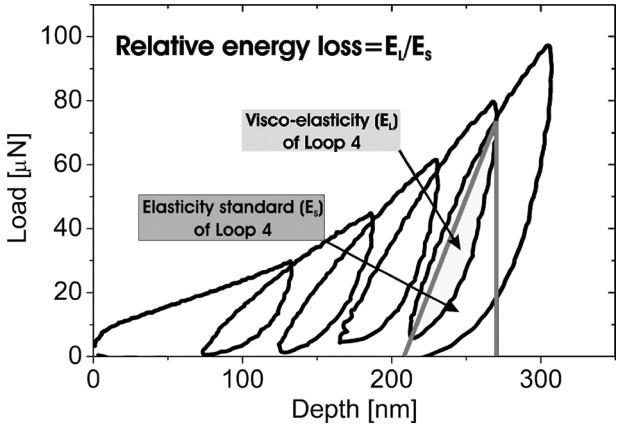

FIGURE 4 Schematic showing the method of calculation for the visco-elastic energy loss from multicycling nanoindentation.

the hardness as a function of penetration depth may be extracted as shown in Figure 3c. Note in Figure 3, that the hardness decreases with increasing penetration depth, as is typically observed in these experiments, but also that the nylon sample exhibits a convex shape during unloading: hysteresis. These loops are indicative, in MPI samples, of visco-elastic energy losses during nanoindentation of the films and are also depth dependent [19,20]. Although such loops complicate the determination of the indentation modulus, which is dependent upon the slope of the unloading curve, they permit analysis of the visco-elastic energy loss itself, see Figure 4. Since the loop size varies with indentation depth, the relative visco-elastic energy loss, E_{loss}, is defined by the ratio of the loop energy, $\mathrm{E_L}$, and the elastic energy, E_{S}, at a particular indentation depth,

$$\mathrm{E_{loss}} = \mathrm{E_L}/\mathrm{E_S}. \tag{3}$$

The visco-elastic energy loss is a characteristic value for the material.

APPLICATION TO NYLON FILMS

The type of analysis described in the previous section has been applied, to differing degrees of completeness, to all three polymer systems shown in Figure 2. Here, we briefly describe the results for the most complete application, to thin nylon films.

Film recognition activity is coordinated with the appearance of nanometer-sized pores in all cases. The nanomechanical properties

of the imprinted network reflect the various functional states of molecularly imprinted polymer films; changes in indentation modulus, hardness and visco-elastic energy loss may be used to distinguish quickly among these different functionalized states. The aim of our investigations is to develop a proper measuring procedure that accounts for the internal relaxation time of the imprinted films, the properties of the functionalized state and the rationale for the observations. We have applied a 12-cycle testing system with parabolically increasing maximum force and 10 s holding times to control, as created, empty and reinserted state nylon films. The force-depth curves reveal significantly different responses to these tests; the actual applied force, the maximum penetration depth and the visco-elastic energy loss reflect the functional state of the MIP and may be readily applied to identify the nature of that state. The results from a series of such studies are shown in Table 1.

The loading of glutamine into nylon based MIP films increases the hardness and the indentation modulus in comparison to pure nylon films. The visco-elastic energy loss is slightly less than in pure nylon films. The removal of the glutamine softens the nylon film, which is evidenced by a decrease in hardness and indentation modulus. The removal process leads to a higher visco-elastic energy loss. Reloading of glutamine results in an increase of the hardness and the indentation modulus to approximately the original values. Again, the visco-elastic energy loss decreases. However, a full reloading of the template to the original status could not be achieved. Loading, removal and reloading of glutamine on the film are clearly measurable with the nanoindentation method. Similar observations may be made from the data in Table 1 for the alanine imprinted MIP. The change in functional state is readily tracked by the nanomechanical properties. However, the smaller size of the alanine molecule appears to enhance

TABLE 1 Nanomechanical Parameters for Nylon-Amino Acid MIPS

Polymer/MIP	State	$\%E_L$	H, GPa	E_R, GPa
Nylon	–	37	0.20	2.2
Nylon-alanine	As produced	35	0.18	3.2
	Template removed	59	0.07	0.09
	Template reinserted	49	0.13	2.1
Nylon-glutamine	As produced	32	0.25	3.7
	Template removed	48	0.16	2.0
	Template reinserted	35	0.23	3.4
	Alanine inserted	43	0.18	2.2

the inability to return these parameters to their as produced values. An interesting experiment documented in Table 1 involves the attempted insertion of alanine into the originally glutamine imprinted film. Alanine is significantly smaller in molecular size and the hydrogen bonding function groups will not align with the respective groups in the nylon cavity. Hence, one expects that alanine will not successfully insert into the film. The data in the table indicate that these expectations were fulfilled and all three values, H, E_R and E_L, are indicative of the template-removed state of the glutamine imprinted film. Initial results consistent with those we have discussed for nylon are also obtained for polyvinylphenol templated with either methyl nitrobenzoate or fructose.

The behavior of the nylon films may be rationalized in terms of a simple model. The elastic behaviour of the material under the indent is a result of the gliding of the aligned (almost linear) nylon chains after the adhesion energy between molecules has been overcome. Twisted nylon molecules (forming the spherical-like cavity) are the basis for the observed visco-elastic effects. These chains are stretched by indentation and may either return to their original conformation or remain in a stretched state as the indenter is unloaded.

A series of simple molecular force field calculations provided information on the chemical basis for the nanomechanical observations. Using three nylon dimers as the host system, two different orientations were obtained as energy minima for the control samples. One consisted of aligned nylon chains and the second was a spherical-like cavity. The linear configuration resulted from an initial state in which the nylon chains were held linear; any initial bending of the chains produced the cavity. Mixed systems of the nylon chains plus amino acid molecule (alanine, glycine or glutamine) yielded nylon-amino acid templated structures. The glutamine structure was a tight cavity with the amino acid firmly locked in to its multiply hydrogen bonded position. The alanine containing cavity was somewhat larger and the amino acid molecules were only hydrogen bonded at one point. Finally, the glycine structure minimized to a linear nylon configuration with the amino acid alternating with the host. One expects, based on these descriptions, a decreasing hardness in the order presented and that is what we have experimentally observed.

POTENTIAL AS SENSORS

Sensors with high specificity, low cost and high sensitivity may be used to detect chemical and biological substances in a wide range of scenarios, including medical diagnostics and threat detection. As is

true for most modern devices, the sensor is expected to be sensitive, miniature, and highly selective. One promising approach is to create a sensing element using nanocapacitive techniques combined with molecularly imprinted films. Such a device would be compatible with industrially-developed miniature transmitters. The potential of using MIPs as the specificity element is clear from our previous discussion. One is left to ponder only the means to detect changes in the functional state of the MIP.

Many creative detection schemes are possible. Perhaps the simplest, and simplicity is a strong value, is to measure a capacitance change due to the presence of the template in the MIP. Capacitive arrangements have been used with MIP layers for a small number of analytical tests, such as for glucose [21] and creatinine [22]. In most of these examples, the sensor has been an exposed electrode in solution, and cyclovoltammetry has been used to determine the behavior of the electrical double layer at the surface. Changes in the dielectric constant of the MIP are then reflected in changes in the capacitance derived from the usual model of the surface charges.

An alternative is a bilayer capacitor in a planar configuration with a grid as the top electrode. MIP sites exposed to the analyte bind the target, leading to a change in capacitance, which reflects the functional state of the material between the electrodes. Such a design leverages capacitive humidity sensors available commercially. With a sensor area of $1\,cm^2$, the capacitance of such a structure is of the order of 5000 pF, which is a readily measurable value. The change due to occupancy of the sites, in a simple-minded calculation, could then be as large as 100 pF. There are several electronic configurations that would allow easy detection; the simplest is to make the sensor part of a resonant circuit, and use a digital counter to measure the frequency.

A sensor scheme, based on recent developments in nanotechnology, is shown in Figure 5. There has been some preliminary work on the use of nanoparticles to detect changes in the chemical environment. The nanoparticles are exposed to various solvents, and resulting changes in the electron transport properties are observed. However, the results obtained so far do not exhibit the high selectivity required for a functional sensor. The experimental conditions were, typically, highly controlled to protect the nanoparticles from extraneous contaminants. Combining the technique with molecular imprint selectivity creates a new generation of sensors. Integration of a nanoparticle layer into the MIP sensor leads to a resistive measurement of the changes induced in the nanoparticle layer. Both dc and resonant circuit methods are applicable for detecting the conductivity change induced by binding the target molecules. The substrate is first

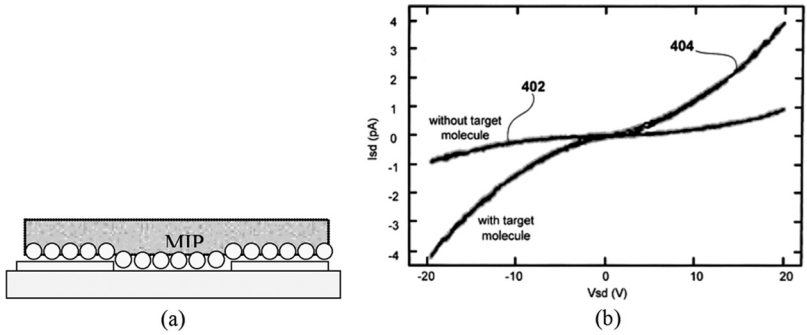

FIGURE 5 Schematic drawing of nanoparticle-MIP sensor described in the text (a) and current vs. voltage plot for such as sensor showing the signal difference for template present and absent (b).

patterned with electrodes, then, the nanoparticle film is be deposited. Polymerization or chemical crosslinking of the nanoparticle arrays is used to stabilize them with respect to the MIP solvents as was the case for the capacitive sensor. The structure for these measurements is shown in Figure 5a. Electrical measurements are made using standard test instrumentation available from the semiconductor industry. One of the critically important questions is the distance over which changes in the local dielectric environment (in the MIP) will affect the transport properties of the nanoparticle array. We have produced a test version of this device that has been shown to indicate the difference between a templated and a control film as shown in Figure 5b. A patent application [23] for such a device has been submitted.

REFERENCES

[1] Haupt, K., Cormack, P. A., & Mosbach, K. (2002). *Biochromatography*, 419.
[2] Ramakrishnan, K. & Prasada, R. (2006). *Separation Science and Technology*, *41*, 233; Xiong, Y., Zhou, H., Zhang, Z., He, D., & He, C. (2006). *The Analyst*, *131*, 829.
[3] Puoci, F., Iemma, F., Cirillo, G., Picci, N., Matricardi, P., Alhaique, F., & Alhaique, F. (2007). *Molecules*, *12*, 805; Cunliffe, D., Kirby, A., & Alexander, C. (2005). *Advanced Drug Delivery Reviews*, *57*, 1836.
[4] Ramstroem, O., Ye, L., Krook, M., & Mosbach, K. (1998). *Chromatographia*, *47*, 465.
[5] Glad, M., Reinholdsson, P., & Mosbach, K. (1995). *Reactive Polymers*, *25*, 47; O'Shannessy, D. J., Andersson, L. I., & Mosbach, K. (1989). *Journal of Molecular Recognition*, *2*, 1.
[6] Ye, L., Ramstroem, O., & Mosbach, K. (1998). *Analytical Chemistry*, *70*, 2789.
[7] Andersson, L. I., Ekberg, B., & Mosbach, K. (1993). *Mol. Interact. Biosep.*, *383*.
[8] Ansell, R. J., Kriz, D., Mosbach, K., & Haupt, K. (1996). *Current Opinion in Biotechnology*, *7*, 89; Kempe, M. & Mosbach, K. (1999). *Tetrahedron Letters*, *36*, 3563; Schillemans, J. P. & van Nostrum, C. F. (2006). *Nanomedicine*, *1*, 437.

[9] Greene, N. T., Morgan, S. L., & Shimizu, K. D. (2004). *Chemical Communications*, *1172*; Stephenson, C. J. & Shimizu, K. D. (2007). *Polymer International*, 56, 482.
[10] Sellergren, B. (2000). *Angewandte Chemie, International Edition*, *39*, 1031.
[11] Sreenivasulu, R. P., Kobayashi, T., & Fujii, N. (2002). *European Polymer Journal*, *38*, 779; Sreenivasulu, R. P., Kobayashi, T., Abe, M., & Fujii, N. (2002). *European Polymer Journal*, *38*, 521.
[12] Wang, H. Y., Xia, S. L., Shao, L., Sun, H., Liu, Y. K., Cao, S. K., & Kobayashi, T. (2004). *Journal of Chromatography B*, *804*, 127; Pang, X., Cheng, G., Li, R., Lu, S., & Zhang, Y. (2005). *Analytica Chimica Acta*, *550*, 13.
[13] Sneshkoff, N., Crabb, K., & BelBruno, J. J. (2002). *Journal of Applied Polymer Science*, *86*, 3611.
[14] Maier, P., Werner-Allen, J., Gibson, U. J., Richter, A., & BelBruno, J. J. (2004). *Surface and Interface Analysis*, *36*, 1340.
[15] Richter, A., Gruner, M., BelBruno, J. J., Gibson, U. J., & Nowicki, M. (2006). *Colloids and Surfaces A*, *401*, 284–285; Richter, A., Gibson, U. J., Nowicki, M., & BelBruno, J. J. (2006). *Journal of Applied Polymer Science*, *101*, 2919.
[16] Fischer-Cripps, A. C. (2004). *Nanoindentation, 2nd Ediiton*, Springer: New York.
[17] Hysitron, Inc. 10025 Valley View Road, Minneapolis, MN 55344 USA.
[18] Oliver, W. C. & Pharr, G. M. (1992). *Journal of Materials Research*, *7*, 1564.
[19] BelBruno, J. J., Richter, A., Campbell, S. E., & Gibson, U. J. (2007). *Polymer*, *48*, 679.
[20] Nowicki, M., Richter, A., Wolf, B., & Kaczmarek, H. (2003). *Polymer*, *44*, 6599.
[21] Chen, G., Sundaresan, V., & Arnold, F. H. (1997). *Polymeric Materials Science and Engineering*, *76*, 378.
[22] Lakshmi, D., Prasad, B., Bali, S., & Piyush, S. (2006). *Talanta*, *70*, 272.
[23] U.S. Provisional Patent Application No. 60/814,021.